Local order and thermal conductivity in yttria-stabilized zirconia. II. Numerical and experimental investigations of thermal conductivity

Mathieu Fèvre* and Alphonse Finel
Laboratoire d'Etude des Microstructures, ONERA, BP72, 29, Avenue de la Division Leclerc, 92322 CHATILLON Cedex, France

René Caudron
Laboratoire d'Etude des Microstructures, ONERA, BP72, 29, Avenue de la Division Leclerc, 92322 CHATILLON Cedex, France and Laboratoire Léon Brillouin, CNRS-CEA, CEA-Saclay, 91191 Gif-sur-Yvette Cedex, France

Rémy Mévrel
Département Matériaux Métalliques et Procédés, ONERA, BP72, 29, Avenue de la Division Leclerc, 92322 CHATILLON Cedex, France
(Received 8 October 2004; revised manuscript received 30 June 2005; published 30 September 2005)

The thermal conductivity of yttria-stabilized zirconias has been determined numerically, by applying a nonequilibrium molecular dynamic calculation. Comparing random configurations and Monte Carlo configurations in which chemical correlations are taken into account, we have established that the short range order developing in yttria-stabilized zirconia gives rise to an increase in lattice thermal conductivity for high dopant concentrations and temperatures below 800 K. At higher temperatures or for lower concentrations, the short range order does not influence the thermal conductivity. This conclusion is consistent with experiment. The results are discussed in relation with the various phonon scattering mechanisms.

DOI: 10.1103/PhysRevB.72.104118 PACS number(s): 61.43.Bn, 02.70.Uu, 02.70.Ns, 61.12.Ex

I. INTRODUCTION

Zirconia ceramics constitute a class of materials of technological and scientific importance, in particular for high temperature applications, such as heat insulation in thermal barrier coatings. Yttria-stabilized zirconias contain a large proportion of point defects, due to the substitution of Zr^{4+} ions with Y^{3+} ions, and the correlated incorporation of oxygen vacancies to preserve the lattice electroneutrality. As shown in Ref. 1, the thermal conductivity of yttria-zirconia systems, with yttria content ranging between 0 and 10 mol % Y_2O_3, can be described within the classical phonon theory provided a critical mean free path is introduced. However, this simple approach cannot be extended to systems having too many point defects and does not explain for example why at room tempertaure the thermal conductivity of yttria-stabilized zirconia, as determined by Bisson *et al.*[2] on single crystals, increases for yttria content above 12 mol % Y_2O_3 (up to 46 mol % Y_2O_3).

The objective of this investigation is to compute the thermal conductivity of these systems with a molecular dynamics technique, and relate the variations in composition and temperature with microstructural features, in particular the short range order characterized both experimentally and with numerical simulation in the companion paper.[3] In Sec. II, the nonequilibrium molecular dynamics method is used to compute the thermal conductivity from atomic configurations. The influence of local order on the thermal transport properties is then discussed in Sec. III.

II. THERMAL CONDUCTIVITY OF YTTRIA DOPED ZIRCONIA

To evaluate the lattice thermal conductivity K, we employed a method based on molecular dynamics calculations. Atomic configurations extracted from Monte Carlo or molecular dynamics simulations are used as a starting point. To determine the conductivity we implemented the nonequilibrium molecular dynamics (NEMD) method into the MOLDY code available at http://www.earth.ox.ac.uk/~keithr/moldy.html.[4] This section briefly presents the NEMD, highlights the influence of atomic interaction potentials on the computed values and compares the calculations to experimental measurements.

A. Technical details

The thermal conductivity tensor $\vec{\vec{K}}$ is related to the energy flux $\vec{J}_E$ and to the applied temperature gradient $\vec{\nabla}T$ by Fourier's law:

$$\vec{J}_E = -\vec{\vec{K}} \cdot \vec{\nabla} T. \tag{1}$$

The expression of the energy flux as a function of atomic variables can be obtained using the energy conservation law, $\dot{H} + \vec{\nabla} \cdot \vec{J}_E = 0$, H being the Hamiltonian of the system.[5] In a classical approach the energy flux takes the form

$$\vec{J}_E(t) = \frac{1}{V}\left\{ \sum_{i=1}^{N} \left(\frac{\vec{p}_i^{\,2}}{2m_i} + \sum_{j \neq i} \phi_{ij} \right) \vec{v}_i - \frac{1}{2} \sum_{i,j=1}^{N} \vec{r}_{ij} (\vec{f}_{ij} \cdot \vec{v}_i) \right\}, \tag{2}$$

where $f_{ij}^a = -d\phi_{ij}/dr_j^a$ is the force between particle i at position $\vec{r}_i$ and particle j at position $\vec{r}_j$, $\vec{p}_i$ is the momentum of particle i and $\vec{r}_{ij} = \vec{r}_j - \vec{r}_i$. V is the system volume and ϕ_{ij} the potential energy between particle i and particle j.

Thermal conductivity can be obtained from molecular dynamics using either equilibrium simulations, based on

Green-Kubo equations, or from steady-state nonequilibrium (NEMD) simulations. The Green-Kubo equations used to calculate the thermal conductivity tensor K^{ab} can be written as follows, in the linear response formalism:

$$K^{ab} = \frac{V}{3k_B T^2} \int_0^\infty d\tau \langle J_E^a(0) J_E^b(\tau) \rangle_{eq}, \tag{3}$$

where $\langle \cdots \rangle_{eq}$ denotes the equilibrium average. Equation (3) shows that the autocorrelation function must be evaluated and integrated over long times, i.e., in a regime where it becomes increasingly difficult to have a good statistics because the autocorrelation function decreases slowly and nonmonotically towards zero. The slow convergence of the integral may then be a problem.

In steady-state nonequilibrium methods, the thermal conductivity is derived from Fourier's law. This can be done by subdividing the simulation box into slabs and imposing a heat flux between cool and hot slabs, thus generating a temperature gradient.[6,7] This method requires large simulation boxes in order to partition the system into a number of slabs where equilibrium can take place, i.e., slabs that contain enough particles for computing average thermodynamic quantities. In addition, instabilities may appear in the neighborhood of the hot and the cool slabs and as a result some slabs cannot be used to compute the heat flux or the temperature gradient. However, this method has been employed for large systems and we will compare the results obtained in Sec. II.[8]

These drawbacks may be overcome with another nonequilibrium molecular dynamics method, the homogeneous field method.[9–11] In this method an external field $\vec{f}_{ext}$ is introduced in Newton's equations so as to produce a desired heat flow:

$$\dot{\vec{p}}_i = \vec{f}_i + \vec{\vec{D}}_i \cdot \vec{f}_{ext}(t), \tag{4}$$

where the tensor $\vec{\vec{D}}_i$, defined as

$$D_i^{ab} = \left(\frac{\vec{p}_i^2}{2m_i} + \phi_i \right) \delta_{ab} - \frac{1}{2} \sum_{j=1}^{N} r_{ij}^a f_{ij}^b + \frac{1}{2N} \sum_{k=1}^{N} \sum_{j=1}^{N} r_{kj}^a f_{kj}^b \tag{5}$$

represents the coupling between the perturbation and the system. Simulations with different values for the external field are performed and the time averaged heat flux $\langle J_E^b \rangle_t$ is calculated. The thermal conductivity is obtained from extrapolation to zero field amplitude:

$$K^{ab} = \lim_{f_{ext} \to 0} \lim_{t \to \infty} \frac{\langle J_E^b \rangle_t}{V T f_{ext}^a(t)}. \tag{6}$$

As this relationship is of the first order in the energy flux J_E, this NEMD method avoids the long computation times that result from the Green-Kubo equation [Eq. (3)] which is of the second order in J_E. In other words, a good statistics is more easily achieved in the NEMD method, because it does not require the computation of fluctuations.

The initial configuration is obtained by a Monte Carlo simulation at $T = 1500$ K, as described in the companion paper.[3] This guarantees that the chemical correlations between ions are reproduced in the initial configuration and that we start, from the chemical point of view, with the correct local order. This cannot be attained by a direct use of molecular dynamics on a totally disordered configuration, where yttrium ions are randomly placed on the cation sublattice and oxygen vacancies on the anion sublattice. This initial Monte Carlo configuration is then equilibrated with the Moldy code, in order to reproduce the lattice vibrations, during 20 ps with a time step of 1 fs. The temperature is then decreased down to 300 K by 100 K steps. At each temperature, the configuration is equilibrated with the same procedure as above (20 ps with 1 fs steps) and the thermal conductivity is calculated with the NEMD method, the mean energy flux being averaged over 20000 time steps. It is to note that Monte Carlo simulations are used only to reach equilibrium at 1500 K. In fact at lower temperature, we know that the local (chemical) order associated with cations does not evolve anymore. Therefore, Monte Carlo simulations are not needed when we proceed below 1500 K. However, the lattice vibrations will still be equilibrated, because they of course do not require diffusion, and molecular dynamics may be used for that purpose. Meanwhile, this procedure is closely related to what is really happening in the samples. Indeed, in the companion paper of this article, we showed that below 1400 K the cations in zirconia can be considered as frozen, the cations diffusion coefficients being very small, and as a consequence, the oxygen ions adapt their movements to the cation positions. In the simulations, the equilibrium state associated to cations corresponds to the Monte Carlo configuration calculated for a temperature of 1500 K and below that temperature, only oxygen ions can diffuse in the molecular dynamics simulations. For configurations associated with Monte Carlo simulations, the equilibrium state related to cations corresponds to the Monte Carlo configuration calculated for a temperature of 1500 K and below that temperature, only oxygen ions can diffuse in the molecular dynamics simulations. In what follows, we call these configurations "Monte Carlo" configurations. For configurations associated with molecular dynamics simulations on disordered systems, yttrium ions are randomly distributed on the cation sublattice and oxygen vacancies have been equilibrated via thermal annealing. We call these configurations "random" or "disordered" configurations in the following.

B. Results: Temperature and concentration dependence of the conductivity

Figure 1 shows the computed conductivity as a function of temperature for two defect concentrations, 8 and 40 mol % Y_2O_3, and for two types of atomic configurations: Monte Carlo configurations where chemical correlations between species are taken into account, and disordered configurations where yttrium ions are randomly distributed. As the classical approach is valid only for temperature well above the Debye temperature, only variations above this temperature (500 K for zirconia), are reported in the graphs. At low defect concentrations, both configurations give similar results, with a thermal conductivity steadily decreasing as a function of temperature. However, at 40 mol % and below

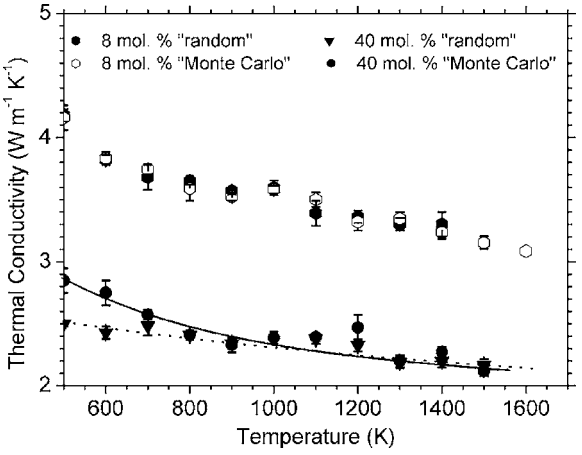

FIG. 1. Temperature dependence of the thermal conductivity of yttria doped zirconia (8 mol % and 40 mol % Y_2O_3), computed using the homogeneous NEMD method. Two atomic configurations are considered: a disordered system ("random") and a system preliminarily equilibrated with Monte Carlo simulations.

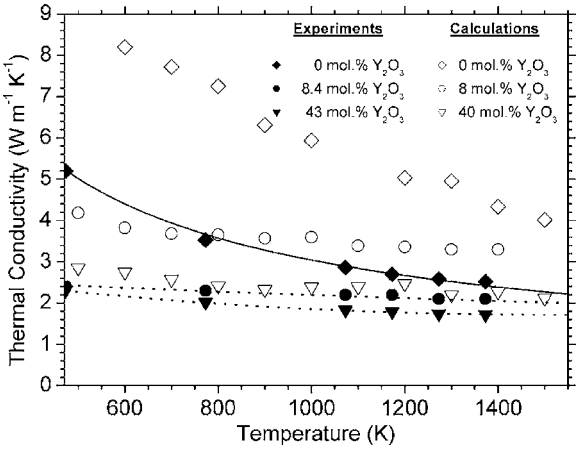

FIG. 2. Temperature and compositions dependence of the thermal conductivity of yttria doped zirconia; computed data with NEMD method and experimental data determined from thermal diffusivity measured by the laser flash method. Lines have been drawn for clarity.

800 K the temperature dependence of the conductivity is more important in the case of Monte Carlo configurations than for random configurations. As discussed in the companion paper,[3] two types of short-range order develop in the Y_2O_3-ZrO_2 system: one related to the tetragonal phase at low defect concentrations and one associated to the δ phase at high doping levels. Fig. 1 indicates that, at low temperature, the thermal conductivity is sensitive to the local order associated with the delta phase, whereas the influence of the tetragonal short range order is negligible at all temperatures. Above around 800 K, the thermal conductivities for both Monte Carlo and disordered configurations are the same. Another important point concerns the accuracy of the calculations within the NEMD method. As shown in Fig. 1, the estimated error bars range from ±0.03 to ±0.15 W m^{-1} K^{-1}. We also note that the statistical fluctuations of the computed values are of the order of 0.1 W m^{-1} K^{-1} i.e. of the same order as the error bars. Thus, the accuracy of the method for the yttria-stabilized zirconia system is below ±0.2 W m^{-1} K^{-1}.

In Fig. 2 thermal conductivity calculations are compared with experimental data obtained on single crystals from thermal diffusivity measurements by the laser-flash technique.[2] For pure zirconia, the strong temperature variations of the experimental thermal conductivity are not correctly reproduced by the calculations. It is to note however that the interatomic potential parameters we used in the calculations stabilize an orthorhombic phase below 1500 K (see companion paper) whereas the equilibrium phase is in fact monoclinic below 1300 K. Increasing the yttria concentration, and as a consequence the point defect content results in less pronounced temperature variations, with similar trends for calculated and experimental data. At high temperature, the experimental conductivity seems to converge towards a value of around 2 W m^{-1} K^{-1}. For these high temperatures, the order of magnitude of the calculated thermal conductivities is close to the experimental values, in particular for highly doped zirconia.

Figure 3 shows the variations of the thermal conductivity as a function of the yttria content at 1500 K for the calculated values and at 1373 K for the experimental data (measurements are described in the next section). The difference between the two sets of data progressively decreases as the yttria content increases. It must be kept in mind that for low yttria content, between 2 and 8 mol % Y_2O_3, the single crystals are two-phase materials (cubic+tetragonal), whereas the simulations correspond to a single cubic phase.

Figure 4 compares the experimental and calculated thermal conductivity as a function of yttria content for temperatures close to the Debye temperature (around 500 K). A rising trend can be seen at high doping concentrations both for the experimental data and for the thermal conductivity calculated from the Monte Carlo configurations. This trend is absent for the variations of the thermal conductivity calculated with the random configurations. This result tends to show that the increase in thermal conductivity observed experimentally at high yttria content might be related to the

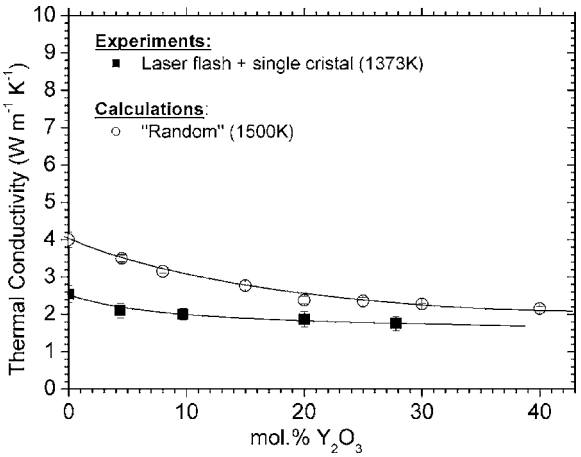

FIG. 3. Concentration dependence of the high temperature thermal conductivity measured by the laser flash technique and computed using the NEMD method.

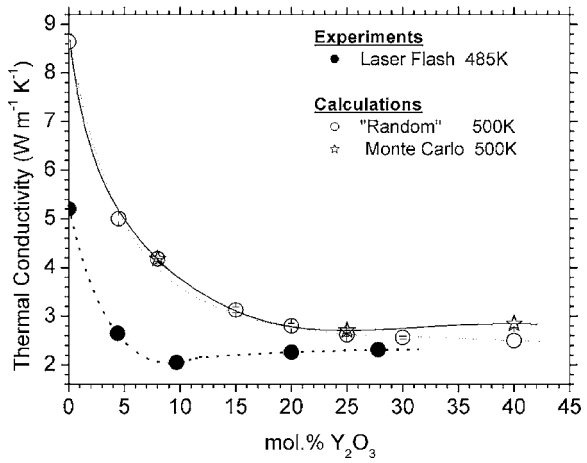

FIG. 4. Concentration dependence of the thermal conductivity measured by the laser flash technique and computed using the NEMD method close to Debye temperature ($T_D \sim 500$ K).

local ordering of point defects at low temperatures, evidenced with the Monte Carlo simulations (see companion paper). However, our calculations were performed within a classical approach and at around 500 K, quantum effects might not be negligible. Further comparison with experiment needs a discussion which is presented in the next section.

C. Quantum effects at low temperatures

In fact, 500 K is indeed close to the zirconia Debye temperature.[12] Due to quantum effects, the actual value of the heat capacity is less than its classical limit and this may be one of the reasons why the computed thermal conductivity is higher than the experimental one (see Fig. 4).

However, this difference could also be due to other effects. It can be argued that the experimental conductivity might be limited by some scattering channels active in a real system and not taken into account in the simulation, such as scattering of phonons by extended defects (dislocations or grain boundaries). However, we first note that the measurements have been done on single crystals and that dislocations are not so numerous in these very ionic solids. Moreover, as discussed below, the mean free path of phonons in our highly disordered systems is actually very small (a few a at most, where a is the lattice parameter). This excludes the influence of extended defects whose average separation is large. Another specific scattering channel has also been proposed to explain the particular behavior of the thermal conductivity of amorphous systems, namely an interaction between phonons and other excitations with two energy levels.[21,22] However, this scattering channel operates only at low temperature, and indeed offers an explanation for the T^2 behavior of the thermal conductivity at very low temperature.

In brief, given these remarks, the discrepancy between the computed and the measured thermal conductivity is likely due to the overestimation of the phonon statistics in our classical molecular dynamics.

Therefore, we now evaluate how the thermal conductivity is overestimated due to the classical approximation. First we can remark that for high dopant concentrations, the temperature dependence of the thermal conductivity is small as shown in Fig. 2. We can thus assume that the dominant processes limiting the thermal conductivity are not the phonon-phonon interactions but the phonon-point defects interactions, suggesting that the phonon mean free paths are correctly described in the simulations whereas the heat capacity factor is not. The correction factor to apply to the thermal conductivity and linked to an erroneous heat capacity can be estimated by the following expression, derived from the phonon gas analogy:

$$K \sim \frac{1}{3} c_v v l, \tag{7}$$

in which v is the sound velocity and l the phonon average mean free path. In the case of cubic zirconia, the heat capacity c_v^{quant} can be evaluated by using an Einstein model for the 6 optical modes and a Debye model for the 3 acoustic ones. The correction factor is given by

$$R = \frac{c_v^{quant}}{c_v^{class}},$$

$$R = \frac{1}{3}\left(\frac{T}{\Theta_L^*}\right)^3 \int_0^{\Theta_L^*/T} \frac{x^4 e^x}{(e^x-1)^2} dx + \frac{2}{3}\left(\frac{T}{\Theta_T^*}\right)^3 \int_0^{\Theta_T^*/T} \frac{x^4 e^x}{(e^x-1)^2} dx + \frac{2}{3}\frac{x_E^2 e^{x_E}}{(e^{x_E}-1)^2}, \tag{8}$$

where Θ_L^* and Θ_T^* are the Debye temperatures associated with the longitudinal and transverse modes:

$$\Theta_L^* = \frac{\hbar}{k_B} v_L (6\pi^2 n_m)^{1/3}, \quad \Theta_T^* = \frac{\hbar}{k_B} v_T (6\pi^2 n_m)^{1/3}, \tag{9}$$

with v_L and v_T being the longitudinal and transverse sound velocities and n_m the number of modes per branch and per volume unit. Using $v_L = 7700$ m s^{-1} and $v_T = 4000$ m s^{-1} from Ref. 13, $\Theta_L^* = 635$ K and $\Theta_T^* = 363$ K. In Eq. (8), $x_E = \Theta_E/T$ with Θ_E the Einstein temperature, which can be estimated from the central frequency ω_E of the optical part of the phonon density of states. Using $\omega_E/2\pi \approx 20$ THz from Refs. 14–16, it comes $\Theta_E = 960$ K. The correction factor to be applied on the simulated thermal conductivity amounts to 0.81 at 500 K, 0.95 at 1000 K and 0.98 at 1500 K. It is to be noted that the yttria dependence of the experimental specific heat is small (less than 10% for yttria varying between 4 and 10 mol % Y_2O_3) and can be neglected in this approach.[17,18] Figure 5 shows that for yttria concentrations larger than 15 mol %, the computed values thus corrected are very close to experiment. Although no experimental data could be obtained in the present study for 40 mol % (inadequate single crystal material), the results obtained by Bisson *et al.*[2] indicate a similar rising trend at 300 K up to 40 mol % as the one observed here at 500 K.

In conclusion, given the uncertainties on the experimental and computed data (both of the order of 0.2 W m^{-1} K^{-1}), the simulated conductivity, corrected for quantum effects, shows a remarkable agreement with the experimental conductivities for yttria concentrations between 15 and 40 mol %. This

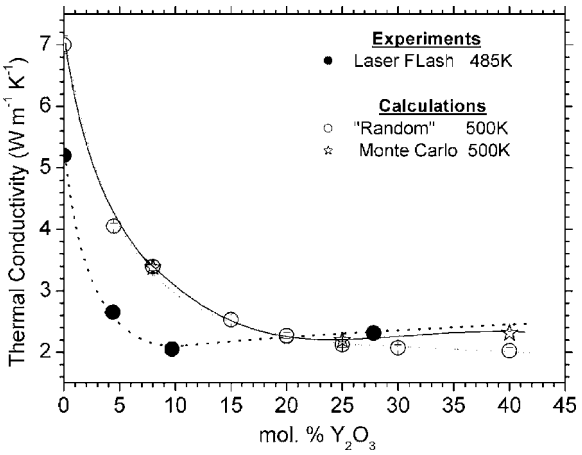

FIG. 5. Concentration dependence of the thermal conductivity measured by the laser flash technique and computed using the NEMD method close to Debye temperature ($T_D \sim 500$ K temperature). Quantum effects are taken into account using the corrective factor R.

clearly demonstrates that the rising trend can be attributed to the local ordering effect evidenced by experiments and simulations in the companion paper. For concentrations below 15 mol %, the discrepancy between simulated and experimental values is likely to arise from the fact that the microstructure cannot be properly reproduced by simulations. In this range of composition, the samples are either in the two-phase domain (tetragonal+cubic) or monoclinic (pure zirconia) whereas the calculated configurations correspond respectively to single cubic or orthorhombic phase.

D. Influence of the box size and interatomic potential

To conclude the presentation of the results obtained with the NEMD homogeneous field method, we examine the sensitivity of the computed conductivities to simulation box size and to interatomic potential parameters that enter the Hamiltonian.

The thermal conductivity of ZrO_2-8 mol % Y_2O_3 has been computed for two systems, one comprising 216 cells (6 cells along each direction) and the other one comprising 504 cells ($7\times8\times9$). It can be seen in Figure 6 that for temperatures above 1000 K, the difference between these two simulations is less than 0.2 W m^{-1} K^{-1}, which is consistent with the simulation accuracy. Figure 7 shows the thermal conductivity of the ZrO_2-8 mol % Y_2O_3 system, computed with two sets of interatomic potential parameters (Brinkman *et al.*,[19] Schelling *et al.*[8]). Considering the values represented by the squares (filled squares for Schelling's parameter set and open squares for Brinkman's set), it appears that similar temperature variations are observed, with a systematic difference of the order of 0.5 W m^{-1} K^{-1}. Calculations done for higher doping concentrations (not reported in the graph of Fig. 7) lead to the same conclusion.[20] In Fig. 7 are also reported the results obtained by Schelling *et al.*[8] by employing the slab method (open circles). The comparison with the results obtained with the NEMD method adopted in the present work indicate a good agreement, with apparently less

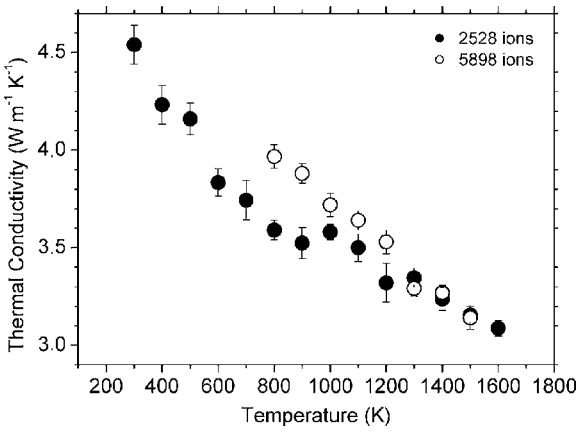

FIG. 6. Influence of simulation box size on computed thermal conductivity of ZrO_2-8 mol % Y_2O_3.

statistical fluctuations for this method, in spite of smaller simulations size boxes (respectively $4\times4\times32$ and $6\times6\times6$ cells).

III. LOCAL ORDER AND THERMAL CONDUCTIVITY IN Y_2O_3-ZrO_2

The results found by NEMD, corrected for quantum effects, are summarized in Fig. 5. Our simulations reproduce the puzzling experimental feature which initially motivated our study: an upturn on the conductivity versus concentration curve at low temperature. Above 20% yttria, this upturn is clearly due to a conductivity which is larger for the Monte Carlo configurations than for the fully disordered configurations. This effect is absent for 8% yttria. These facts, established by numerical simulations may be explained qualitatively and we will also discuss the temperature dependence of the thermal conductivity.

The thermal conductivity of a zirconia system is related to the scattering of phonons by other phonons (via Umklapp processes) and by point defects. These scattering mechanisms can be characterized by phonon mean free paths and the correct physical picture will emerge from the interplay

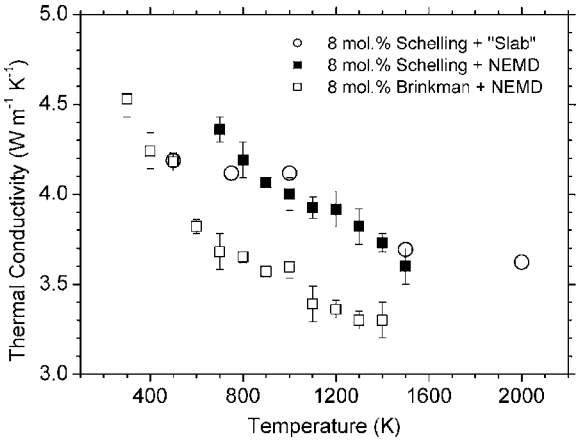

FIG. 7. Influence interatomic potential sets on computed thermal conductivity. See text for details.

between the characteristic lengths of the microstructure, i.e., the correlation length and the average distance between neighboring point defects d_P.

For the temperatures envisaged in the present work, the phonon mean free path for Umklapp processes, l_U, is a strongly decreasing function of temperature. However, it cannot be less than the shortest interatomic distance. On the other hand, the phonon mean free path associated with scattering of phonons by point defects is temperature independent and is related to d_P, the average distance between two neighboring point defects.

For high yttria content (40 mol % Y_2O_3), we have seen (Fig. 1) that, at relatively low temperatures (below 800 K), the computed thermal conductivity for the Monte Carlo configuration is larger than that for the random configuration, indicating that the local order present in the Monte Carlo configurations plays a role in this case. In the random configuration, the average distance between two neighboring vacancies, which rules the phonon mean free path, can be calculated by

$$d \sim \frac{a}{2}\left[\frac{x}{2(1+x)}\right]^{-1/3}, \tag{10}$$

where x is the molar concentration in Y_2O_3. It is of the order of $0.95a$, a being the lattice parameter of the disordered cubic phase. In the Monte Carlo configuration, which exhibits local order, the correlation length can be estimated to $2a$ by extrapolating the values of the correlation lengths found on the diffuse scattering patterns of the companion paper for 9.7 mol % Y_2O_3 and 27 mol % Y_2O_3. This is larger than the average distance between neighboring vacancies ($0.95a$). In this situation, phonons interact with groups of correlated defects rather than individual defects, and the conductivity is higher than in the fully disordered case. At high temperature, the effect of the short range order is negligible, because the phonon scattering is dominated by the Umklapp processes. As expected, with a common value at high temperature and a difference at low temperature, the temperature dependence of the conductivity should be steeper in the short range ordered state than in the fully disordered state.

Explaining why, at low doping concentrations, the thermal conductivity is insensitive to short range order is more difficult because, in this concentration range, the diffuse scattering patterns exhibit two types of short range order, having each their own correlation length. One of them, already mentioned for higher concentrations, is reminiscent of the δ-type order. The other one is associated to the tetragonal phase. However, the nature of these two phases is different: the δ-type order is due to the arrangement of vacancies, whereas the tetragonal phase can be described as displacements of oxygen columns. The latter type of defects is expected to be much less efficient for phonon scattering. This is corroborated by the thermal conductivity measurements we performed on the 9.7 mol % Y_2O_3 sample in the as received state and in an annealed state at 750 °C during 8 months [see Fig. 6(b) of the companion paper]: the results were undistinguishable. So, we are authorized to ignore the tetragonal-like short range order. The order of magnitude of the δ-type correlation length is the same as for the 9.7% case, i.e., $0.9a$, but the average distance between defects, evaluated by Eq. (10), is around $1.5a$. Thus, defects are almost uncorrelated and we can assume that they act individually on phonons (the correlation length has no meaning if smaller than the interdefect distance). So, whatever the temperature, the short range order does not change the thermal conductivity. The temperature dependence of the conductivity, shared by the two states (with short range order and with a random distribution of defects), is naturally steeper than in the concentrated case, as the temperature dependent Umklapp processes are more important than the defect scattering.

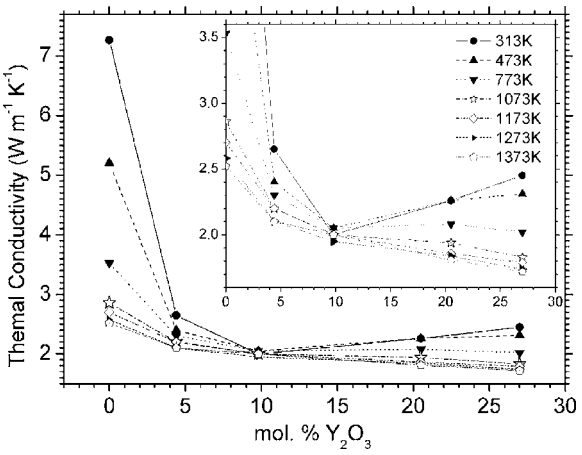

FIG. 8. Evolution of thermal conductivity of yttria-zirconia single crystals as a function of yttria concentration and temperature. Lines have been drawn for clarity. The inset is simply a zoom of the main figure.

Calculations on Monte Carlo configurations showed that the conductivity increases with defect concentration for yttria-rich compositions and for temperatures below 800 K, whereas at high temperature, the conductivity decreases for all the doping concentrations. To our knowledge, no measurements have been published on the yttria-rich compositions, especially at high temperature. To check the predictions of the calculations, we performed some measurements on single crystals for various temperatures. The thermal conductivity has been determined from the thermal diffusivity obtained with a laser-flash method, the experimental specific heat capacity reported in Ref. 1 and the density measured by helium pycnometry. The uncertainty associated with these measurements has been estimated to 8% in relative (see Appendix for experimental details). Results are presented in Fig. 8. Consistently with what we have outlined above, at low temperature, the short range order induces a conductivity increase at high doping, but not at moderate concentrations. This effect no longer exists at high temperature as pointed out by the calculations.

IV. CONCLUSION

We calculated the thermal conductivity of yttria stabilized zirconias by molecular dynamics, as a function of composition (0% to 40 mol % Y_2O_3) and temperature up to 1500 K.

The empirical potentials adopted in this study were sufficient to account for both temperature and concentration behavior. The main results are as follows:

Globally, the trends are consistent with experimental results obtained on single crystals. At moderate temperature (between 300 K and 800 K), the rising trend of the thermal conductivity above 10 mol % Y_2O_3 is correctly described provided a simple quantum correction is applied to the classical results obtained with MD. This rising trend is due to the local ordering of defects and well rendered in the Monte Carlo configurations (see companion paper) used as a starting point in the calculations.

For low yttria concentrations and moderate temperatures, the discrepancy between calculated and experimental results is attributed in part to the fact that the small box size in the computation cannot render the two-phase domain.To have a better description would also imply using a more complex interatomic potential, at the expense of simplicity.

At high temperature ($T > 800$ K), the thermal conductivity variations are dominated by Umklapp processes and the short range order no longer has any detectable influence.

ACKNOWLEDGMENTS

This work has been done in part within the program of international collaboration between the National Science Foundation (DMR-0099695) and the European Commission (GRD2-200-30211). M. Poulain is gratefully acknowledged for preparing the single crystalline samples and characterizing their density. We thank particularly J.-C. Laizet and D. Demange for measuring the thermal diffusivities.

APPENDIX: THERMAL DIFFUSIVITY MEASUREMENTS

For measuring the thermal diffusivity, a single pulse (duration: 3 to 5 ms; energy: 5 J) from a CO_2 laser (wavelength: 10.6 μm) was directed on one face of a disc (10 mm diameter, 1 to 2 mm thick) placed inside a high temperature furnace (atmosphere: argon). The laser pulse is absorbed at the surface of the zirconia-based materials, which have an absorption edge in the range 5–7 μm. An HgCdTe infrared detector was used to measure the temperature from the rear face of the specimens. An optical long-wave pass filter which eliminates the wavelengths shorter than 8 μm was interposed between the back face of the specimens and the detector to suppress radiation coming from within the zirconia material. Thus the radiation recorded by the detector comes only from the back surface of the specimen. With this arrangement, no opaque coating is needed on either face of the specimen, as employed in general for measuring the thermal diffusivity of semitransparent materials. The variations of back-surface temperature as a function of time are analyzed by a method which takes into account radiation and convection losses. Each value of diffusivity represents the average on 4 to 6 measurements.

The single crystals investigated, supplied by Zirmat Corp. (North Billerica), were produced by skull melting crystal growth. More details on the experimental methodology can be found in Ref. 1, which reports and discusses the thermal conductivity measurements on the yttria-poor single crystals (0, 4.4 and 9.8 mol % Y_2O_3). To our knowledge, no measurement has been published on the yttria-rich compositions (20.6 and 27 mol % Y_2O_3).

*Electronic address: Mathieu.Fevre@onera.fr

[1] R. Mévrel, J.-C. Laizet, A. Azzopardi, B. Leclercq, M. Poulain, O. Lavigne, and D. Demange, J. Eur. Ceram. Soc. **24**, 3081 (2004).
[2] J. Bisson, D. Fournier, M. Poulain, O. Lavigne, and R. Mévrel, J. Am. Ceram. Soc. **83**, 1993 (2000).
[3] M. Fèvre, A. Finel, and R. Caudron, preceding paper, Phys. Rev. B **72**, 104117 (2005).
[4] K. Refson, *MOLDY* (Department of Earth Sciences, University of Oxford, London, 1996).
[5] R. Hardy, Phys. Rev. **132**, 168 (1963).
[6] F. Müller-Plathe, J. Phys. C **106**, 6082 (1997).
[7] P. Jund and R. Jullien, Phys. Rev. B **59**, 13707 (1999).
[8] P. Schelling, S. Phillpot, and D. Wolf, J. Am. Ceram. Soc. **84**, 1609 (2001).
[9] D. Evans and G. Morris, *Statistical Mechanics of Non Equilibrium Liquids* (Academic Press, London, 1990).
[10] D. Evans, in *International School of Physics Enrico Fermi*, edited by G. Ciccotti and W. Hoover (Societa Italianà di physica, Bologna, Italy, 1985), p. 221.
[11] S. Motoyama, Y. Ichikawa, Y. Hiwatari, and A. Oe, Phys. Rev. B **60**, 292 (1999).
[12] T. Shirakami, T. Tojo, T. Ataka, T. Mori, and H. Yamamura, Thermochim. Acta **267**, 415 (1995).
[13] F. J. Walker and A. C. Anderson, Phys. Rev. B **29**, 5881 (1984).
[14] M. Ozawa, S. Suzuki, C.-K. Loong, and J. Nipko, Appl. Surf. Sci. **121/122**, 133 (1997).
[15] S. Fabris, A. T. Paxton, and M. W. Finnis, Phys. Rev. B **61**, 6617 (2000).
[16] P. Schelling and S. Phillpot, J. Am. Ceram. Soc. **84**, 2997 (2001).
[17] B. Leclercq, Ph.D. thesis, Université de Limoges, 2002.
[18] S. Raghavan, H. Wang, R. Dinwiddie, W. Porter, and M. Mayo, Scr. Mater. **39**, 1119 (1998).
[19] H. Brinkman, W. Briels, and H. Verweij, Chem. Phys. Lett. **247**, 386 (1995).
[20] M. Fèvre, Ph.D. thesis, Université de Paris XI, 2003.
[21] P. Anderson, B. Halperin, and C. Varma, Philos. Mag. **25**, 1 (1972).
[22] W. Phillips, J. Low Temp. Phys. **7**, 351 (1972).